Scientific Research Publishing

Computational Chemistry, 2017, 5, 74-90
http://www.scirp.org/journal/cc
ISSN Online: 2332-5984
ISSN Print: 2332-5968

Theoretical Investigation of the Newly Designed Benzimidazole Based Metal Mediated DNA Base Couples with DFT Method

Fatma Sevin*, Mostafa Asghari Dilmani, Kübra Sarıkavak, Samira Farshbaf Jeddi

Chemistry Department, Faculty of Science, Hacettepe University, Ankara, Turkey
Email: sevin@hacettepe.edu.tr

How to cite this paper: Sevin, F. Dilmani, M.A., Sarıkavak, K. and Jeddi, S.F. (2017) Theoretical Investigation of the Newly Designed Benzimidazole Based Metal Mediated DNA Base Couples with DFT Method. *Computational Chemistry*, **5**, 74-90.
https://doi.org/10.4236/cc.2017.52007

Received: February 7, 2017
Accepted: April 27, 2017
Published: April 30, 2017

Abstract

DNA has the genetic information storage and transmission capacity according to the sequential order of the monomer and creates a central role in the chemical evolution by copying itself with the proliferation feature. Watson-Crick base pairs define two base pairs with hydrogen bonds. If metal coordination bonds replace hydrogen bonds more stable alternative metallo-DNA sequence can be established. If the replication feature can be obtained for the metallo-DNA, this will greatly benefit the creation of DNA computer keys. In this study, a new type of benzimidazole based metallo-DNA sensors consisting of a connector unit that unsaturated azinil bridge linked to Watson-Crick base pairs with Ni^{2+}, Hg^{2+}, Zn^{2+}, Ag^{+}, Pt^{2+}, Pd^{2+} metal cations and a benzimidazole has been designed. Absorption and emission spectrum of the newly designed aqua medium based fluorophore and their metallo-DNA sensors with selected cations have been theoretically investigated by using DFT method. The logic gates of selected possible sensors which response in the visible region have also been examined in detail in acidic and water phase. As a result of calculated absorption-emission spectrum data show that T-Hg-A-Bnz, A-Ni-T-Bnz, C-Pt-G-Bnz, C-Ni-C-Bnz complexes produce OR gate. T-Zn-T-Bnz and G-Pt-C-Bnz results demonstrated XOR and AND logic gate, respectively.

Keywords

Flourescence, Metallo-DNA Sensor, Benzimidazole, Logic Gates, DFT

1. Introduction

Today, development of biomolecular structures is generally based on supra-molecules that include non-covalent interactions, such as hydrogen bonds, hydrophobic effects and metal coordination bonds [1] [2] [3] [4]. Without a

doubt, the most basic structures in origins of the chemical evolution are the nucleic acids. The most basic indicators that allow storing, transferring and copying of the genetic information within these nuclear acids are hydrogen bonded Watson-Crick base pairs. Having metal coordination bonds instead of hydrogen bonds presents alternative and completely different base pairs [5] [6] [7]. As known, the event of binding a metal ion to a molecule affects the characteristics of UV-visible spectrum of molecule. Fluorescence technics are also good tool to identify biomolecular interactions and uses widely in many research. For these technics, some fluorophores have been used to analyze cations and anions that can be found in the nature. Among various fluorophores, benzimidazole has drawn attention due to its optical properties and high stability. Benzimidazole ring is a very good type of fluorophore as it can produce "scorpion type" complexes [8].

Theoretically suggested one dimensional TMn (benzimidazole)$_{n+1}$ (TM = Sc, Ti, V, Cr, Mn) system's electronic and magnetic characteristics were investigated with DFT method [9]. It was detected that benzimidazole can be stable while also retaining the helix and one-dimensional characteristics of the DNA with the Ti, V and Cr transition atoms. Experimentally [10] and theoretically [11] studies were established about structural-electronic characteristics and UV absorption spectrums of the Thymine-Hg^{2+}-Thymine base pair (T-Hg-T), which is a mercury (II) linked metallo-DNA complex. In the experimental study, the stability of the thymine pair with the mercury ion was determined in various temperatures and pH's and it was seen that its maximum absorption was at 260 nm. In the theoretic study, the base pairs and dimers that thymine and its derivatives of cis and trans form with the mercury ion were calculated with the TD-B3LYP and TD-PCM-B3LYP methods, it was determined that maximum absorption occurs in values that are closer to red, which is to say 263 nm in solvent phase and 276 nm in gas phase.

Takezawa and Shionoya presented an abstract about the chemistry of metal-linked base pairs which includes primary approaches to the DNA based molecular systems, molecular designs,structures, characteristics and their applications in their research [12]. One of the examples that were provided Cu^{2+} linked hydroxipyron base pair. The H-Cu^{2+}-H base pair has a square planar characteristic while H defines a nucleoacid that carries a hydroxipyron. The most distinctive characteristic of the metallo-base pairs added to the DNA is their potential to increase the duplex stability. As expected, metal coordination bond energies are two or three times greater than the hydrogen bonds. For this reason, their stability effects are worked out from the melting temperatures of the DNA base pairs. An example for this is as the following: when there is a Cu^{2+} ion, this temperature has increased from 37˚ Celsius to 50˚ Celsius. Similar stabilities are also achieved in Salen-type. Structures like similar to these are synthesized and characterized as monomer structures at first and then they were added to, for example, 15-mer DNA duplexes. Also, Li *et al.* have examined the aggregation behavior of the silver molecules with the DFT method by using

polymorphic DNA models that contain Watson-Crick base pairs, i-motif and G-quadrulex [13]. Leutwyler group examined double hydrogen bonded complexes of 2-pyridones cytosine and 1-methyl cytosine with mass, UV and IR spectroscopic techniques and observed five different cytosine 2-pyridone isomers in their theoretical and experimental study [14].

Usage of sensors as logic gates in biochemical researches has begun only recently, but it has started developing [15] [16]. In chemical logic systems, binding a guest molecule to the host molecule corresponds to a logical input and the result includes physical changes as an output which corresponds to absorption or fluorescence spectrum. Whenever multiple chemical inputs provide a single output independent of each other, the system is defined as OR logic gates, which is to say that this is a very weak chemical selection system. On the other hand, AND logic gate identifies multiple chemical inputs based on luck and it provides an input that requires high chemical selectivity.

In this study, metallo-DNA sensors that have new fluorescent characteristics and the capability to work in aqueous mediums have been designed by binding metals (Hg^{2+}, Ag^{+}, Ni^{2+}, Pb^{2+}, Pt^{2+}, Zn^{2+}) that can provide them coordination, *especially planar coordination*, to Watson-Crick base pairs and their reversible and changeable optical characteristics in acidic mediums have been investigated and possible logic gates have been suggested. As it can be seen on **Figure 1** and **Figure 2**, a new type of benzimidazole based metallo-DNA base pair sensors have been designed which consisting of a connector unit and unsaturated azinil bridge linked to Watson-Crick (T = Thymine, A = Adenine, C = Cytosine and G = Guanine) base pairs bonded with Ni^{2+}, Hg^{2+}, Zn^{2+}, Ag^{+}, Pt^{2+}, Pd^{2+} metal cations and a fluorophore. These newly designed metallo-sensors have the characteristic that allows molecular identification with visible changes in color (colorimeter) and increases and decreases in emission wavelength (fluorescence) due to their coordination with various cations.

To explain the structural and electronic characteristics of these sensors in different media, their energies, absorption and emission spectrums, energy

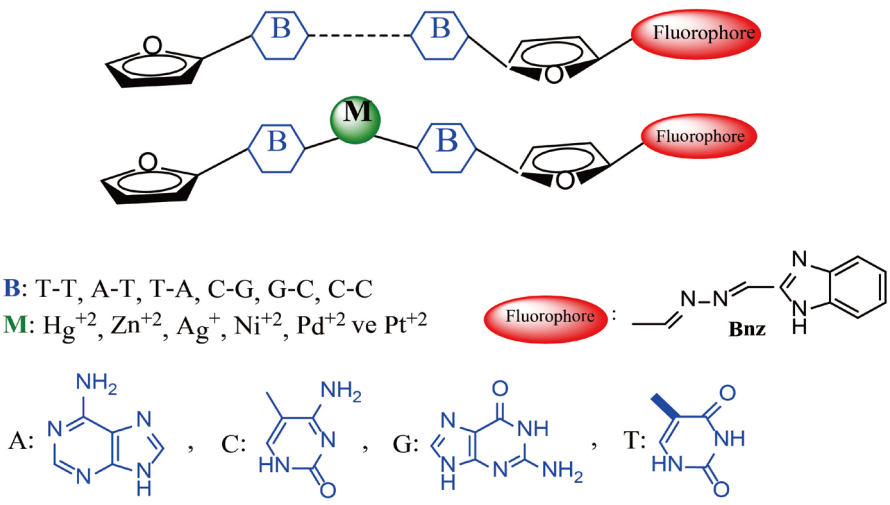

Figure 1. Designed benzimidazole based metallo-DNA based pair sensors.

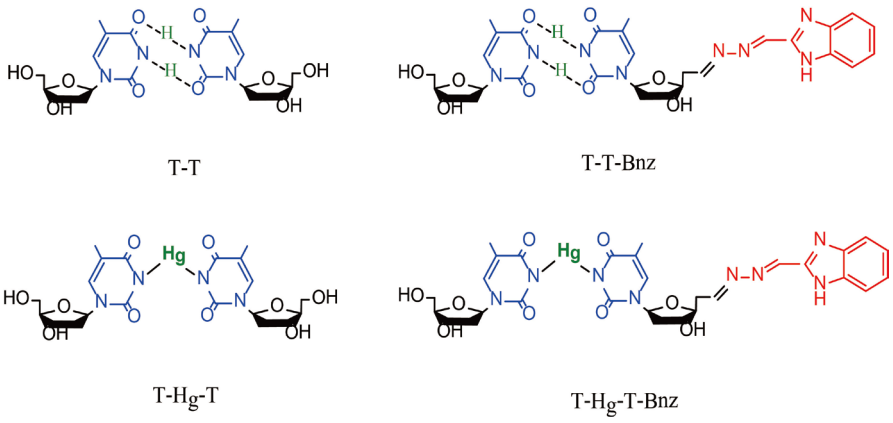

Figure 2. Some azinil benzimidazole mediated tymine base pair examples.

differences between frontier molecular orbitals (HOMO: highest occupied molecular orbital and LUMO: lowest unoccupied molecular orbital) which means HOMO-LUMO gap has been calculated as well as color and emission changes. Same calculations have been made with protonation of sp2 hybrid nitrogen atom of benzimidazole portions and logic gates have been presented for acidic medium and aqueous phase. As a result, since these designed sensors are expected to be potential keys for the DNA computer technology, we expect them to contribute greatly to science and technology applications.

2. Method

In this study, all the calculations have been performed with Gaussian 09W [17] and GaussView 5.0.8 molecular modeling software [18]. The methods used in the calculation of the organometallic compounds with mercury in the literature have been chosen [19] [20] [21]. It is especially known, M06 is one of the best functional for the study of organometallic and inorganomatellic thermochemistry and noncovalent interactions. In the frame of these informationsM06 (Hybrid meta exchange-correlation functionals) [22], B3LYP (Becke, three-parameter, Lee-Yang-Parr) [23], PBE0 (Perdew, Burke and Ernzerhof) [24] methods and the double-zeta pseudo-potential LandL2DZ [25] basis set has been selected for geometry optimization and evaluate the absorption and emission spectroscopy. The selection of appropriate method among the aforecited methods has been based on the experimental results of T-Hg^{2+}-T base pair which has a known maximum absorption value in the literature as 260 nm. These calculated absorption results have been compared with the corresponding experimental values. The calculation results show that M06 functional has been found better than the other methods as in **Table S1** (it is given in Supporting info). After determining the appropriate method, all subsequent calculations performed with M06 functional LandL2DZ basis set. Vibrational frequency analyses have been carried out to confirm local minima of the structures. In order to compute the solvation effect self-consistent reaction field (SCRF) theory with polarizable continuum method (PCM) used in the water phase calcultaions. The dielectric constant was chosen as the standard value for water, (ε = 78.39). Calculations

corresponding to acidic medium implemented with nitrogen protonation of benzimizadole fragment. Absorption and emission spectra calculated and logic gates determined through these constructions.

The total energy of the structures (E), Gibbs free energy (G) and enthalpy (H) has been calculated. Along with gas phase calculation, Conductor-Like Screening Model [26] has been used to calculate theoretical absorption wavelength in aqueous media. Also, 7-digit TD-DFT method has been used for emission calculation [27].

3. Results and Discussion

Investigation of the DNA bases and their structures with metal and benzimidazole has been divided into two categories as T-A, A-T, C-G and G-C base combinations. All calculations have been conducted in the water phase. Formation energies, frontier molecular orbital band gaps have been calculated and studies particularly have focused on the photophysical properties.

3.1. Properties of Designed T-T and T-A and T-A Base Pairs and Their Benzimidazole Base Pairs with and without Metal Cations

In the first stage, the complexation energies of T-T, T-A and A-T base pairs with metal cations have been calculated and obtained results given in **Table 1**. Also, total energies and entaphy have been demonstrated in **Tables S2-S4**. Complexation energies of benzimidazole (Bnz) based T-T,T-A and A-T base pairs with metal cations have been calculated and results given in the same table. As can be seen from the table, complexation of T-T occurs easily with Ni^{2+}. This sequence followed by Hg^{2+}. The complexation abilities of metal cation in this sequence for T-T is $Ni^{2+} > Hg^{2+} > Zn^{2+} > Ag^{+} > Pt^{2+} > Pd^{2+}$. This sequence is the

Table 1. The complexation energies of T-T, T-A and A-T base pairs with metal cations and Bnz (Kcal/mol).

Base Pairs	Energy Values				
	ΔG	Base Pairs	ΔG	Base Pairs	
T-T → T-Hg-T	−122.66	T-A → T-Hg-A	-101.32		
T-T → T-Zn-T	−98.06	T-A → T-Zn-A	−81.46		
T-T → T-Ag-T	−78.26	T-A → T-Ag-A	−72.19		
T-T → T-Ni-T	−183.55	T-A → T-Ni-A	−134.85		
T-T → T-Pd-T	−59.08	T-A → T-Pd-A	−50.00		
T-T → T-Pt-T	−71.98	T-A → T-Pt-A	−61.35		
T-A-Bnz → T-Hg-A-Bnz	96.05	A-T-Bnz → A-Hg-T-Bnz	−105.22	T-T-Bnz → T-Hg-T-Bnz	−112.08
T-A-Bnz → T-Zn-A-Bnz	−77.00	A-T-Bnz → A-Zn-T-Bnz	−84.92	T-T-Bnz → T-Zn-T-Bnz	−99.02
T-A-Bnz → T-Ag-A-Bnz	−64.22	A-T-Bnz → A-Ag-T-Bnz	−76.00	T-T-Bnz → T-Ag-T-Bnz	−79.37
T-A-Bnz → T-Ni-A-Bnz	−122.41	A-T-Bnz → A-Ni-T-Bnz	−104.55	T-T-Bnz → T-Ni-T-Bnz	−184.62
T-A-Bnz → T-Pd-A-Bnz	−45.89	A-T-Bnz → A-Pd-T-Bnz	−54.02	T-T-Bnz → T-Pd-T-Bnz	−60.81
T-A-Bnz → T-Pt-A-Bnz	−56.00	A-T-Bnz → A-Pt-T-Bnz	−67.26	T-T-Bnz → T-Pt-T-Bnz	−73.26

same with T-T for T-A base pair, too.

Complexation of benzimidazole with T-T base pair and its complexation energies with metal cations prefers the Ni^{2+} cation. Its sequence is as following: $Ni^{2+} > Hg^{2+} > Zn^{2+} > Ag^{+} > Pt^{2+} > Pd^{2+}$. T-A-Bnz base pair shows the same trend. This sequence is the same as T-T and benzimidazole did not have an impact on adenine.

It is clearly observed from the results, benzimidazole based A-T designed base pair results show that when benzimidazole bonds with the thymine part of this base pair, the first two rows of the sequence slightly changes: $Hg^{2+} > Ni^{2+} > Zn^{2+} > Ag^{+} > Pt^{2+} > Pd^{2+}$. It can be considered that benzimidazole has more effects on thymine. The result shows that, with the exception of the A-T-Bnz base pair which prefers Hg^{2+} cation, other benzimidazole based DNA base pairs primarily prefer Ni^{2+} cation.

The energy gap reflects the reactivity or stability of the molecule. HOMO-LUMO energy gap of molecules is considered as a measure of charge transfer and is regarded as an important parameter in determining the properties such as electrical conductivity. Table 2 shows that T-T-Bnz has made it stable than T-T about 0.35 eV. However, in case of complexation with metal cations, Pd^{2+} and Pt^{2+} is more thermodynamically stable while the gap energies of other metal cations decrease. This situation shows that conjugation is also increased on the structure. The highest amount conjugation occurs with Ni^{2+} and Ag^{+}among the selected cations. Hence, HUMO-LUMOs of T-Ag-T seen that the contribution of metal orbitals is greater in linked benzimidazole and conjugation shifts to benzimidazole ring. The significant effect has not been observed by linking benzimidazole for T-A base pairs. Complexation energies with $Pd^{2+}$and Pt^{2+} metal cations are higher than the cations for T-A and also with Hg^{2+} and Zn^{2+} cations are decreased their gap energies. In terms of A-T base pairs, bonding of benzimidazole to structure increases molecular stability about 0.20 eV. Although Ag^{+} and Ni^{2+} cations more stable in case of complexation with metal cations, the energy gap values have decreased only for Hg^{2+} cation. Thus, base pair orbitals in T-Hg-T HOMO-LUMOs show benzimidazole orbitals in LUMO when benzimi-

Table 2. The HOMO-LUMO band gap energies of T-T-, T-A and their complexes with Bnz metal cations (eV).

Base Pairs	HOMO-LUMO gap energies						
	-	Hg	Zn	Ag	Ni	Pd	Pt
T-T	1.178	4.602	4.124	4.736	4.649	0.824	0.926
T-T-Bnz	1.552	3.050	3.107	3.009	3.013	0.912	2.354
T-T/T-T-Bnz	−0.347	1.552	1.017	1.727	1.636	−0.088	−1.428
T-A	0.940	3.432	3.785	3.230	3.263	3.395	3.671
T-A-Bnz	0.980	1.413	1.392	4.565	4.763	4.680	4.884
T-A/T-A-Bnz	−0.040	2.019	2.393	−1.335	−1.500	−1.285	−1.213
A-T	0.940	3.432	3.785	3.230	3.263	3.395	3.671
A-T-Bnz	1.139	1.337	4.372	4.566	4.120	3.517	4.227
A-T/A-T-Bnz	−0.199	2.095	−0.587	−1.336	−0.857	−0.122	−0.556

Table 3. Maximum absorption/emission wavelength (nm) and differences between them of the designed T-T, T-A, A-T pairs and their Bnz complexes.

Pairs	T-T- Based					T-T-Bnz Based				
	λ Abs	Osc	λ Ems	Osc	$\Delta\lambda$	Pairs λ Abs	Osc	λ Ems	Osc	$\Delta\lambda$
T-T	264	0.060	293	0.020	28	T-T-Bnz	319	0.620	337	0.430	18
T-Hg-T	335	0.230	397	0.110	43	T-Hg-T-Bnz	358	0.560	407	0.380	49
T-Zn-T	460	0.100	471	0.080	10	T-Zn-T-Bnz	468	0.009	482	0.005	13
T-Ag-T	586	0.010	709	0.009	122	T-Ag-T-Bnz	741	0.090	808	0.070	67
T-Ni-T	283	0.004	314	0.001	31	T-Ni-T-Bnz	331	0.046	359	0.019	105
T-Pd-T	866	0.003	901	0.001	34	T-Pd-T-Bnz	967	0.001	1109	0.008	141
T-Pt-T	603	0.025	738	0.013	13	T-Pt-T-Bnz	807	0.078	921	0.047	113
	T-A- Based					T-A-Bnz Based				
T-A	301	0.030	339	0.028	38	T-A-Bnz	334	0.060	357	0.051	22
T-Hg-A	473	0.047	509	0.044	35	T-Hg-A-Bnz	468	0.019	509	0.016	41
T-Zn-A	602	0.051	668	0.040	65	T-Zn-A-Bnz	692	0.029	715	0.017	23
T-Ag-A	645	0.088	861	0.082	216	T-Ag-A-Bnz	781	0.067	898	0.056	116
T-Ni-A	343	0.027	457	0.023	114	T-Ni-A-Bnz	351	0.004	477	0.003	126
T-Pd-A	864	0.002	985	0.001	121	T-Pd-A-Bnz	986	0.058	1108	0.054	121
T-Pt-A	767	0.700	789	0.650	21	T-Pt-A-Bnz	801	0.061	827	0.540	26
	A-T- Based					A-T-Bnz Based				
A-T	301	0.030	339.	0.028	38	A-T-Bnz	365	0.013	404	0.012	38
A-Hg-T	473	0.047	509	0.044	35	A-Hg-T-Bnz	439	0.019	488	0.014	48
A-Zn-T	602	0.051	668	0.040	65	A-Zn-T-Bnz	658	0.020	670	0.018	12
A-Ag-T	645	0.088	861	0.082	216	A-Ag-T-Bnz	772	0.060	893	0.056	121
A-Ni-T	343	0.027	457	0.023	114	A-Ni-T-Bnz	443	0.002	661	0.002	217
A-Pd-T	864	0.002	985	0.001	121	A-Pd-T-Bnz	822	0.001	1043	0.001	221
A-Pt-T	767	0.700	789	0.650	21	A-Pt-T-Bnz	789	0.670	839	0.590	40

dazole enters. According to calculations; Hg^{2+}, Ag^{+} and Zn^{2+} cations can increase resonance stability of structure and Pt^{2+} and Pd^{2+} cations provides thermodynamic stability.

In the scope of this section, absorption and emission spectrum has been studied and results of the complexes formed by T-T, T-A, A-T bases and their benzimidazole based pairs with metals has been given in Table 3. This table shows that T-T-Bnz and T-M-T complexes have maximum absorption and emission wavelength (λ_{max}) with Zn^{2+} and Ag^{+} cations, respectively. For Ag^{+} cations, Stokes shift value are greater than Zn^{2+} cations. When the results are evaluated for T-A and T-A-Bnz, it has seen that maximum absorption and emission wavelength λ_{max} values belong to T-Hg-A, T-Zn-A and T-Zn-A–Bnz complexes. $\Delta\lambda$ value of the T-A based complex with Ni^{2+} cations is higher than Hg^{2+} cations one. The results obtained by A-T based structures are the same with the obtained for T-A structure. Maximum absorption and emission wavelength for A-T-Bnz belong to the A-Zn-T-Bnz complex

In accordance with spectral data of T-T, T-A, A-T base pairs with selected

metals and benzimidazole their colors have been determined before and after radiation. The color difference caused by the binding of metal cations to T-T and T-T-Bnz structures is given in the Table S5. The color change from blue to green has been observed in T-Hg-A, T-Zn-T-Bnz, A-Hg-T and T-Hg-A-Bnz complexes. The color change from violet to green has been seen in A-Hg-T-Bnz and A-Ni-T-Bnz pairs. Yellow coloured T-Ag-T and orange coloured T-Pt-T base pairs has losts their colours after radiation like red coloured T-Ag-A, T-Zn-A-Bnz and A-Ag-T pairs. T-Ni-A, T-Ni-A-Bnz and A-Ni-T complexes that are colourless initially,have gained blue colour after radiation. Colorless A-T-Bnz and T-Hg-T-Bnz pairs have gained violet colour, too. The color change from yellow to red has been observed for T-Ag-T and A-Zn-T pairs

3.2. Properties of Designed C-G and G-C Base Pairs and Their Benzimidazole Base Pairs with and without Metal Cations

As in the previous section, complexation energies, band gaps and spectral properties of the targeted structures has been studied in this part, too. Table 4 displays complexation energies of C-G and C-C base pairs and their combinations with benzimidazole and selected cations.

Calculations show that the complexation of C-G and C-C occurs easily with Ni^{2+} like T-T and A-T ba-ses. The metal cation sequence for C-G is $Ni^{2+} > Hg^{2+} > Pt^{2+} > Pd^{2+} > Ag^{+} > Zn^{2+}$. The metal cation sequence for C-C is $Ni^{2+} > Ag^{+} > Hg^{2+} > Zn^{2+} > Pd^{2+} > Pt^{2+}$. Unlike the others, this sequence is followed by Ag^{+}. When the complexation energies analyzed for created by complexation of Bnz based C-G pairs with metal cations, it has been seen that the bonding of Bnz with guanine is the same as its bonding with G-C base pair and this has not changed the preference of it. The same results have been obtained for G-C-Bnz complex and C-C-Bnz complex. The results of all the complexation calculations

Table 4. The complexation energies of C-G -Bnz and G-C-Bnz base pairs with metal cations (Kcal/mol).

Base Pairs	Energy Values				
	ΔG	Base Pairs	ΔG	Base Pairs	
C-G → C-Hg-G	−140.33	C-C → C-Hg-C	−91.33	C-G-Bnz → C-Hg-G-Bnz	
C-G → C-Zn-G	−63.55	C-C → C-Zn-C	−82.22	C-G-Bnz → C-Zn-G-Bnz	
C-G → C-Ag-G	−77.77	C-C → C-Ag-C	−94.27	C-G-Bnz → C-Ag-G-Bnz	
C-G → C-Ni-G	−154.64	C-C → C-Ni-C	−110.01	C-G-Bnz → C-Ni-G-Bnz	
C-G → C-Pd-G	−101.04	C-C → C-Pd-C	−80.00	C-G-Bnz → C-Pd-G-Bnz	
C-G → C-Pt-G	−113.36	C-C → C-Pt-C	−79.88	C-G-Bnz → C-Pt-G-Bnz	
G-C-Bnz → G-Hg-CBnz	−132.45	C-C-Bnz → C-Hg-CBnz	−132.45	C-G-Bnz → C-Hg-G-Bnz	−125.05
G-C-Bnz → G-Zn-C-Bnz	−69.01	C-C-Bnz → C-Zn-C-Bnz	−69.01	C-G-Bnz → C-Zn-G-Bnz	−61.04
G-C-Bnz → G-Ag-C-Bnz	−81.34	C-C-Bnz → C-Ag-C-Bnz	−81.34	C-G-Bnz → C-Ag-G-Bnz	−73.24
G-C-Bnz → G-Ni-C-Bnz	−150.09	C-C-Bnz → C-Ni-C-Bnz	−150.09	C-G-Bnz → C-Ni-G-Bnz	−147.69
G-C-Bnz → G-Pd-C-Bnz	−99.58	C-C-Bnz → C-Pd-C-Bnz	−99.58	C-G-Bnz → C-Pd-G-Bnz	−94.26
G-C-Bnz → G-Pt-C-Bnz	−110.78	C-C-Bnz → C-Pt-C-Bnz	−110.78	C-G-Bnz → C-Pt-G-Bnz	−104.97

Table 5. The HOMO-LUMO band gap energies of C-G, C-C and their complexes with Bnz and metal cations (eV).

Base Pairs	HOMO-LUMO gap energies						
	-	Hg	Zn	Ag	Ni	Pd	Pt
C-G	1.573	1.629	3.198	1.201	1.814	2.329	0.825
C-G-Bnz	0.973	0.630	3.489	2.708	2.046	3.470	3.476
C-G/C-G-Bnz	0.600	0.999	−0.291	−1.507	−0.232	−1.141	−2.651
G-C	1.573	1.629	3.198	1.201	1.814	2.329	0.825
G-C-Bnz	0.580	2.319	3.452	3.078	3.342	3.211	3.188
G-C/G-C-Bnz	0.993	−0.690	−0.254	−1.877	−1.528	−0.882	−2.363
C-C	0.829	2.377	3.800	2.977	2.993	2.979	2.998
C-C-Bnz	0.914	2.051	3.652	2.029	2.916	3.274	2.706
C-C/C-C-Bnz	−0.085	0.326	0.148	0.948	0.077	−0.295	0.292

shows that except for A-T-Bnz base pair which prefers Hg^{2+} cation, other benzimidazole based DNA base pairs primarily prefer Ni^{2+} cation. Also, the HOMO-LUMO band gaps of the molecules can be seen in Table 5. It is observed from Table 5 binding benzimidazole to C-G has created 0,60 eV of conjugation andthis effect has been found for the Hg^{2+} cation while the band gap of other cations has in-creased. The greatest difference has been observed with Pt^{2+} cation. Binding of Bnz to G-C provides 0.993 eV of resonance stability. However, when complexation occurs with other metal cations, gap energy values have increased and this value is greater than what is for Pt^{2+} cation. Binding benzimidazole to C-C does not bring about a large effect and it is complexed with any metal cation other than Pd^{2+}, gap energy value decreases and this decrease is greater than the decrease for Ag^{+}. All the results related to band gaps show that resonance stability is increased with Hg^{2+}, Ag^{+} and Zn^{2+} while thermodynamic stability is increased with Pt^{2+} and Pd^{2+} cations.

The absorption and emission spectrum has been studied and results of the complexes have been formed by C-G, C-G and C-C bases and benzimidazole based pairs with metals have been given in Table 6.

According to Table 6, maximum absorption and emission wavelength values have been calculated for the Pt^{2+} cation, which is the most probable cation for both C-M-G and C-M-G-Benzimidazole complexes. The results gathered for G-C based structures are the same with the data which obtained by C-G pair. Examination of the maximum absorption and emission values in the visible area shows that the biggest $\Delta\lambda$ value belongs to the C-Ni-C and C-Ni-C-Bnz complexes.

Base pairs that show whatsoever colour change has been determined as in the previous section. Colour changes of the base pairs depending on before and after radiation has been presented in Table S9. As can be seen, colour changes of C-M-G and C-M-G-Bnz pairs are same with G-M-C and G-M-C-Bnz pairs because of absorption and emission wavelength of these pairs have equal values. Red coloured C-Hg-C, C-Ag-C and Bnz pairs have disappeared colour. A similar situation has occurred in blue coloured C-Pt-G and violet coloured C-Ni-C base

Table 6. Maximum absorption/emission wavelength (nm) and differences between them of the designed C-G, G-C, C-Cpairs and their Bnz complexes.

Pairs	C-G- Based					C-G-Bnz Based				
	λ Abs	Osc	λ Ems	Osc	$\Delta\lambda$	Pairsλ	Abs	Osc	λ Ems	Osc	$\Delta\lambda$
C-G	263	0.037	294	0.020	30	C-G-Bnz	297	0.005	310	0.005	13
C-Hg-G	324	0.024	450	0.170	126	C-Hg-G-Bnz	349	0.020	462	0.016	112
C-Zn-G	830	0.020	1047	0.015	216	C-Zn-G-Bnz	799	0.020	921	0.017	122
C-Ag-G	794	0.045	815	0.030	21	C-Ag-G-Bnz	743	0.038	761	0.039	18
C-Ni-G	297	0.026	514	0.025	217	C-Ni-G-Bnz	311	0.005	735	0.004	423
C-Pd-G	473	0.026	491	0.024	18	C-Pd-G-Bnz	479	0.007	491	0.006	11
C-Pt-G	454	0.029	789	0.026	334	C-Pt-G-Bnz	439	0.006	663	0.006	194
	G-C- Based					G-C-Bnz Based					
G-C	263	0.037	294	0.020	30	G-C-Bnz	279	0.015	290	0.014	10
G-Hg-C	324	0.024	450	0.170	126	G-Hg-C-Bnz	376	0.015	597	0.011	220
G-Zn-C	830	0.020	1047	0.015	216	G-Zn-C-Bnz	784	0.012	891	0.011	107
G-Ag-C	794	0.045	815	0.030	21	G-Ag-C-Bnz	718	0.081	774	0.079	56
G-Ni-C	297	0.026	514	0.025	217	G-Ni-C-Bnz	293	0.098	417	0.086	178
G-Pd-C	473	0.026	491	0.024	18	G-Pd-C-Bnz	468	0.076	489	0.075	21
G-Pt-C	454	0.029	789	0.026	334	G-Pt-C-Bnz	403	0.006	615	0.005	212
	C-C Based					C-C-Bnz Based					
C-C	398	0.001	419	0.001	21	C-C-Bnz	343	0.001	374	0.001	31
C-Hg-C	699	0.019	742	0.018	42	C-Hg-C-Bnz	693	0.014	711	0.012	18
C-Zn-C	778	0.002	797	0.002	18	C-Zn-C-Bnz	722	0.003	775	0.002	52
C-Ag-C	670	0.009	985	0.008	314	C-Ag-C-Bnz	691	0.014	813	0.012	122
C-Ni-C	403	0.014	729	0.012	326	C-Ni-C-Bnz	414	0.016	635	0.012	220
C-Pd-C	775	0.017	892	0.011	117	C-Pd-C-Bnz	751	0.008	860	0.005	108
C-Pt-C	786	0.086	802	0.070	16	C-Pt-C-Bnz	769	0.023	781	0.021	11

pairs. Blue-green change exhibited in C-Pd-G and its benzimidazole pair. Violet coloured C-Pt-G-Bnz, G-Pt-C-Bnz and C-Ni-C-Bnz pairs have changed their colours to red, orange and again orange, respectively. Colourless pairs C-Hg-G and its Bnz pair has turned their colour to blue while C-Ni-G green.

3.3. Logic Gates

The most probable DNA base pairs with and without metal cations that could be demonstrate Stokes shift has been selected for logic gate calculations. Acidic media effect is included by the protonation of the nitrogen atom on benzimidazole fragment. For this purpose, a proton has been linked to the nitrogen atom of benzimidazole and calculated their absorption and emission spectrums aqueous phase. The results of the selected T-Zn-T, T-Hg-A, A-Ni-T, C-Pt-G, G-Pt-C and C-Ni-C base pairs have been given in the Table 7 and Table 8.

Examination of the tables show that T-Hg-A, A-Ni-T, C-Pt-G, C-Ni-C base pairs represents an OR logic gate, while T-Zn-T, G-Pt-C produces AND gate and XOR gate, respectively. In the AND gate for T-Zn-T pair, fluorescence takes

Table 7. Logic Gates for T-T, T-A, A-T base pairs and their complexes with Bnz.

Pairs	λ Abs (nm)	λ Ems (nm)	Δλ (nm)	Input H^+	Input Zn^+	Input Hg^{2+}	Input Ni^+	Output AND	Output OR	λ Max (nm)
T-T-Bnz	319	337	18.23	0	0			0		337.73
T-H^+-T-Bnz	517	531	24.81	1	0			0		531.34
T-Zn-T-Bnz	468	482	13.60	0	1			0		482.10
T-Zn,H^+-T-Bnz	843	912	91.02	1	1			1		912.80
									0	
T-A-Bnz	334	357	22.87	0		0			1	357.04
T-H^+-A-Bnz	412	431	54.18	1		0			1	431.13
T-Hg-A-Bnz	468	509	41.68	0		1			1	509.08
T-Hg,H^+-A-Bnz	574	581	73.20	1		1				581.34
A-T-Bnz	365	404	38.69	0			0		0	404.40
A-H^+-T-Bnz	487	356	43.26	1			0		1	536.38
A-Ni-T-Bnz	443	661	217.40	0			1		1	661.20
A-Ni,H^+-T-Bnz	364	381	57.05	1			1		1	381.09

Table 8. Logic Gates for C-G, G-C, C-C base pairs and their complexes with Bnz.

Pairs	λ Abs (nm)	λ Ems (nm)	Δλ (nm)	Input H^+	Input Pt^+	Input Ni^+	Output OR	Output XOR	λ Max (nm)
C-G-Bnz	297	310	13.77	0	0		0		310.80
C-H^+-G-Bnz	363	401	74.43	1	0		1		401.06
C-Pt-G-Bnz	439	663	194.76	0	1		1		663.76
C-Pt,H^+-G-Bnz	812	940	217.60	1	1		1		940.62
G-C-Bnz	279	290	10.38	0	0			0	290.03
G-H^+-C-Bnz	964	1012	148.90	1	0			1	1012.1
G-Pt-C-Bnz	403	615	212.16	0	1			1	615.2
G-Pt,H^+-C-Bnz	321	340	29.03	1	1			0	340.6
C-C-Bnz	343	374	31.53	0		0			374.60
C-H^+-C-Bnz	363	382	37.66	1		0			382.17
C-Ni-C-Bnz	414	635	220.34	0		1			635.24
C-Ni,H^+-C-Bnz	276	616	89.47	1		1			316.43

place when the proton and the Zn^{2+} cation available in the system at the same time. XOR gate for G-Pt-C occurs in the event of being proton or Pt^{2+} cation. For the afore-mentioned other base pairs have shown OR logic gateand it means that fluorescence can be seen when the metal cation, proton and both of them are in the system.

Also, bonding of metal cation and protonation of selected pairs has been caused to red shift in absorption spectrum as well as emission spectrum for all the interested base pairs. C-Ni-C-Bnz pair shows the most largest Stokes shift among the molecules that have been selected for logic gates calculations. The C

and G base pairs have higher Stokes shift values than the thymine and adenine pairs.

4. Conclusion

In this study, we have theoretically studied complexation energies, their band gap and electronic absorption-emission spectral behaviors of targeted DNA base pairs in the water phase. In order to determine the appropriate method for UV-vis absorption wavelength maxima of pairs, it has been calculated with three different functionals and compared with the experimental data and each other. Results show that M06/Lanl2dz level is good agreement with experimental absorption wavelength. The energy calculation results give that all the base pairs primarily prefer Ni^{2+} cation for complexation, whereas A-T base pairs prefer Hg^{2+} cation. The same trend has been observed in case of being benzimidazole in pairs. HOMO-LUMO band gap results have shown that the resonance stability increased with Hg^{2+}, Ag^{+} and Zn^{2+} cations, while the Pt^{2+} and Pd^{2+} provide thermodynamically stable. Our calculated electronic spectrum presents that designed DNA base pairs can be use as a probe to detected selected cations. The fluorescence of C-G, G-C pairs answers for $Pt^{2+,}$ Pd^{2+} and Zn^{2+} cations, while T-T, T-A and A-T are given for Hg^{2+}, Ag^{+} and Zn^{2+} cations. The calculated results for their logic gates have been given that addition of protons to designed DNA pairs causes a red shift for all pairs in the water phase. Also, the presence of metal cations causes a red shift like protonation, except for Ni^{2+} cation. As a result of calculated absorption-emission spectrum data show that T-Hg-A-Bnz, A-Ni-T-Bnz, C-Pt-G-Bnz, C-Ni-C-Bnz complexes produce OR gate. T-Zn-T-Bnz and G-Pt-C-Bnz results demonstrated XOR and AND logic gate, respectively. In brief, this theoretical study manifestes important electronic and photophysical behaviors of designed metallo-DNA pairs which can be use to determining of selected cations.

Acknowledgements

We acknowledge the support of TUBITAK (Scientific and Technical Research Council of the Turkish Republic) under grant no. 214Z022.

References

[1] Holliday, B.J. and Mirkin, C.A. (2001) Strategies for the Construction of Supramolecular Compounds through Coordination Chemistry. *Angewandte Chemi*, **40**, 2022-2043. http://dx.doi.org/10.1002/1521-3773(20010601)40:11<2022::AID-ANIE2022>3.0.CO;2-D

[2] Panja, K.S., Dwivedi, N. and Saha, S. (2016) Highly Stable Naphthalene Core Based Novel Cleftshaped Strain Molecule: Influence of Intermolecular H-Bonding Architectures. *The Royal Society of Chemistry*, **6**, 59574-59581. http://dx.doi.org/10.1039/c6ra06855c

[3] Mahmudov, K.T., Kopylovich, M.N., Silva, F.C. and Pombeiro, A.J.L. (2016) Non-Covalent İnteractions in the Synthesis of Coordination Compounds: Recent Ad-

vances. *Coordination Chemistry Reviews*.
http://dx.doi.org/10.1016/j.ccr.2016.09.002

[4] Hisamatsu, Y., Miyazawa, Y., Yoneda, K., Miyauchi, M., Zulkefeli, M. and Aoki, S. (2016) Supramolecular Complexes Formed by the Self-Assembly of Hydrophobic Bis(Zn2+-cyclen) Complexes, Copper, and Di- or Triimide Units for the Hydrolysis of Phosphate Mono- and Diesters in Two-Phase Solvent Systems (Cyclen = 1,4,7,10-Tetraazacyclododecane). *Chemical and Pharmaceutical Bulletin*, **64**, 451-464. http://dx.doi.org/10.1248/cpb.c15-01014

[5] Smith, S.J., Radford, R.J., Subramanian, R.H., Barnett, B.R., Figueroa, J.S. and Tezcan, F.A. (2016) Tunable Helicity, Stability and DNA-Binding Properties of Short Peptides with Hybrid Metal Coordination Motifs. *Chemical Science*, **7**, 5453-5461. http://dx.doi.org/10.1039/c6sc00826g

[6] Santamaria-Diaz, N., Mendez-Arriaga, M.J., Salas, J.M. and Galindo, M.A. (2016) Highly Stable Double-Stranded DNA Containing Sequential Silver (I)-Mediated 7-Deazaadenine/Thymine Watson-Crick Base Pairs. *Angewandte Chemie*, **55**, 6170-6174. http://dx.doi.org/10.1002/anie.201600924

[7] Léon, J.C., Sinha, I. and Müller, J. (2016) 6-Pyrazolylpurine as an Artificial Nucleobase for Metal-Mediated Base Pairing in DNA Duplexes. *International Journal of Molecular Sciences*, **17**, 554-564. http://dx.doi.org/10.3390/ijms17040554

[8] Camacho, C.C., Ruiz, A.E., Hueso P.A., Mijangos, E., Garcia, I.R., Contreras, R. and Parra, A.F. (2013) Organometallic Tin Compounds Derived from 2-Benzimidazole Propionic Acid. *Zeitschrift für anorganische und allgemeine Chemie*, **7**, 1122-1128. http://dx.doi.org/10.1002/zaac.201300108

[9] Mallajosyula, S.S. and Pati, S.K. (2008) Benzimidazole-Modified Single-Stranded DNA: Stable Scaffolds for 1-Dimensional Spintronics Constructs. *Journal of Physical. Chemistry B*, **112**, 16982-16989. http://dx.doi.org/10.1021/jp8080782.

[10] Miyake, Y., Togashi, M., Tashiro, M., Yamaguchi, H., Oda, S., Kudo, M., Tanaka, Y., Kondo, Y., Sawa, R., Fujimoto, T., Machinami, T. and Ono, A. (2005) Mercury^{II}-Mediated Formation of Thymine-Hg^{II}-Thymine Base Pairs in DNA Duplexes. *Journal of the American Chemical Society*, **128**, 2172-2173. http://dx.doi.org/10.1021/ja056354d

[11] Miyachi, H., Matsui, T., Shigetac, Y. and Hirao, K. (2009) Effects of Mercury (II) on Structural Properties, Electronic Structure and UV Absorption Spectra of a Duplex Containing Thymine-Mercury(II)-Thymine Nucleobase Pairs. *Physical Chemistry Chemical Physics*, **12**, 909-917. https://doi.org/10.1039/B912807G

[12] Takezawa, Y. and Shıonoya, M. (2012) Metal-Mediated DNA Base Pairing: Alternatives to Hydrogen-Bonded Watson Crick Base Pairs. *Accounts of Chemical Research*, **45**, 2066-2076. https://doi.org/10.1021/ar200313h

[13] Wu, J., Fu, Y., He, Z., Han, Y., Zheng, L., Zhang, J. and Li, W. (2012) Growth Mechanisms of Fluorescent Silver Clusters Regulated by Polymorphic DNA Templates: A DFT Study. *The Journal of Physical Chemistry B*, **116**, 1655-1665. https://doi.org/10.1021/jp206251v

[14] Müller, A., Talbot, F. and Leutwyler, S. (2002) Hydrogen Bond Vibrations of 2-Aminopyridineâ2-Pyridone, Watson-Crick Analogue of Adenine Uracil. *Journal of the American Chemical Society*, **124**, 14486-14494. https://doi.org/10.1021/ja0209969

[15] Brown, G.J. (2004) Encyclopedia of Supramolecular Chemistry. In: Atwood, J.L. and Steed, J.W., Eds., *Encyclopedia of Supramolecular Chemistry*, CRC Press, Taylor and Francis Group, New York, 893.

[16] Kubo, K. (2005) PET Sensors. In: Geddes, C.D. and Lakowicz, J.R., Eds., *Topics in*

Fluorescence Spectroscopy: *Advanced Concepts in Fluorescence Sensing*, Springer Science Business Media, New York, 241.

[17] Frisch, M.J., Trucks, G.W., Schlegel, H.B., Scuseria, G.E., Robb, M.A., Cheeseman, J.R., Scalmani, G., Barone, V., Mennucci, B., Petersson, G.A., Nakatsuji, H., Caricato, M., Li, X., Hratchian, H.P., Izmaylov, A.F., Bloino, J., Zheng, G., Sonnenberg, J.L., Hada, M., Ehara, M., Toyota, K., Fukuda, R., Hasegawa, J., Ishida, M., Nakajima, T., Honda, Y., Kitao, O., Nakai, H., Vreven, T., Montgomery, J.A., Peralta, J.E., Ogliaro, F., Bearpark, M., Heyd, J.J., Brothers, E., Kudin, K.N., Staroverov, V.N., Kobayashi, R., Normand, J., Raghavachari, K., Rendell, A., Burant, J.C., Iyengar, S.S., Tomasi, J., Cossi, M., Rega, N., Millam, J.M., Klene, M., Knox, J.E., Cross, J.B., Bakken, V., Adamo, C., Jaramillo, J., Gomperts, R., Stratmann, R.E., Yazyev, O., Austin, A.J., Cammi, R., Pomelli, C., Ochterski, J.W., Martin, R.L., Morokuma, K., Zakrzewski, V.G., Voth, G.A., Salvador, P., Dannenberg, J.J., Dapprich, S., Daniels, A.D., Farkas, Ö., Foresman, J.B., Ortiz, J.V., Cioslowski, J. and Fox, D.J. (2009) Gaussian 09, Revision E.01. Gaussian Inc., Wallingford.

[18] Dennington, R., Keith, T. and Millam, J. (2009) Gauss View.

[19] Zhang, B., Ma, P., Gao, D., Wang, Z., Sun, Y., Song, D. and Li, X. (2016) A FRET-Based Fluorescent Probe Formercury Ions in Water and Living Cells. *Spectrochimica Acta Part A*: *Molecular and Biomolecular Spectroscopy*, **165**, 99-105.

[20] Sicilia, V., Borja, P., Bayab, M. and Casasb, J. (2015) Selective Turn-Off Phosphorescent and Colorimetric Detection of Mercury (II) in Water ByhalfLantern Platinum(II) Complexes. *Dalton Transactions*, **44**, 6936-6943. https://doi.org/10.1039/C5DT00087D

[21] Karhu, A., Rautiainen, M., Oilunkaniemi, R., Chivers, T. and Laitinen, R. (2015) Mercury- and Cadmium-Assisted [2 + 2] Cyclodimerization of Tert-Butylselenium Diimide. *Inorganic Chemistry*, **54**, 9499-9508. https://doi.org/10.1021/acs.inorgchem.5b01434

[22] Zhao, Y. and Truhlar, D.G. (2006) The M06 Suite of Density Functionals for Main Group Thermochemistry, Thermochemical Kinetics, Noncovalent Interactions, Excited States and Transition Elements: Two New Functionals and Systematic Testing of Four M06-Class Functionals and 12 Other Functionals. *Theoretical Chemistry Accounts*, **120**, 215-241. https://doi.org/10.1007/s00214-007-0310-x

[23] Rives, J.T. and Jorgensen, W.L. (2008) Performance of B3LYP Density Functional Methods for a Large Set of Organic Molecules. *Journal of Chemical Theory and Computation*, **4**, 297-306. https://doi.org/10.1021/ct700248k

[24] Adamo, C. and Barone, V. (1999) Toward Reliable Density Functional Methods without Adjustable Parameters: The PBE0 Model. *The Journal of Chemical Physics*, **113**, 6158-6170. https://doi.org/10.1063/1.478522

[25] Chiodo, S., Russo, N. and Sicilia, E. (2006) LANL2DZ Basis Sets Recontracted in the Framework Of Density Functional Theory. *The Journal of Chemical Physics*, **125**, 104-107. https://doi.org/10.1063/1.2345197

[26] Klamt, A. (1994) Conductor-Like Screening Model for Real Solvents: A New Approach to the Quantitative Calculation of Solvation Phenomena. *The Journal of Physical Chemistry*, **99**, 2224-2235. https://doi.org/10.1021/j100007a062

[27] http://www.gaussian.com/g_tech/g_ur/k_scrf.htm

Supplementary Tables

Table S1. HOMO-LUMO molecular orbital energies and complexation energies in eV for T-Hg-T, calculated with MO6, B3LYP and PBE0 method (Kcal/mol).

Methods	T-Hg-T						
	HOMO	LUMO	ΔGap(L-H)	ΔG	ΔH	ΔE	Absorbance
B3LYP	−6.46	−1.15	5.30	−595906.58	−595862.38	−595874.80	269.34
PBE0	−5.56	−1.78	5.78	−595417.20	−595373.64	−595386.05	331.99
M06	−6.76	−0.95	5.81	−595556.71	−595513.17	−595525.35	264.48

Table S2. The complexation energies of thymine-thymine (T-T), thymine-adenine (T-A) base pairs with metal cations (Kcal/mol).

Base Pairs	Energy Values						
	ΔE	ΔG	ΔH	Base Pairs	ΔE	ΔG	ΔH
T-T→ T-Hg-T	−113.11	−122.66	−122.64	T-A → T-Hg-A	−97.02	−101.32	95.98
T-T→ T-Zn-T	−89.06	−98.06	−88.49	T-A → T-Zn-A	−77.75	−81.46	−77.02
T-T→ T-Ag-T	−69.98	−78.26	−69.69	T-A → T-Ag-A	−64.99	−72.19	−61.76
T-T→ T-Ni-T	−147.64	−183.55	−143.50	T-A → T-Ni-A	−123.26	−134.85	−119.63
T-T→ T-Pd-T	−52.12	−59.08	−51.23	T-A → T-Pd-A	−47.78	−50.00	−47.22
T-T→ T-Pt-T	−63.41	−71.98	−61.54	T-A → T-Pt-A	−56.36	−61.35	−54.49

Table S3. The complexation energies of T-T-Bnz and T-A-Bnz base pairs with metal cations (Kcal/mol).

	Energy Values						
Base Pairs	ΔE	ΔG	ΔH	Base Pairs	ΔE	ΔG	ΔH
T-T-Bnz → T-Hg-T-Bnz	−112.91	−112.08	−112.53	T-A-Bnz → T-Hg-A-Bnz	−97.02	−96.05	−94.01
T-T-Bnz → T-Zn-T-Bnz	−89.37	−99.02	−88.62	T-A-Bnz → T-Zn-A-Bnz	−77.75	−77.00	−75.67
T-T-Bnz → T-Ag-T-Bnz	−70.01	−79.37	−69.91	T-A-Bnz → T-Ag-A-Bnz	−64.99	−64.22	−60.80
T-T-Bnz → T-Ni-T-Bnz	−147.98	−184.62	−143.72	T-A-Bnz → T-Ni-A-Bnz	−123.26	−122.41	−121.33
T-T-Bnz → T-Pd-T-Bnz	−52.18	−60.81	−51.39	T-A-Bnz → T-Pd-A-Bnz	−47.78	−45.89	−45.46
T-T-Bnz → T-Pt-T-Bnz	−63.74	−73.26	−62.35	T-A-Bnz → T-Pt-A-Bnz	−56.36	−56.00	−55.03

Table S4. The complexation energies of A-T-Bnz base pairs with metal cations (Kcal/mol).

Base Pairs	Energy Values		
	ΔE	ΔG	ΔH
A-T-Bnz → A-Hg-T-Bnz	−101.11	−105.22	−98.88
A-T-Bnz → A-Zn-T-Bnz	−83.10	−84.92	−83.00
A-T-Bnz → A-Ag-T-Bnz	−71.26	−76.00	−69.77
A-T-Bnz → A-Ni-T-Bnz	−102.95	−104.55	−100.00
A-T-Bnz → A-Pd-T-Bnz	−51.01	−54.02	−50.13
A-T-Bnz → A-Pt-T-Bnz	−63.53	−67.26	−63.06

Table S5. The colour changes of of T-T, T-A, A-T and their complexes with Bnz and metal cations.

T-M-T	B.L	A.L	T-M-T-Bnz	B.L	A.L
T-T	-	-	T-T-Bnz	-	-
T-Hg-T	-	-	T-Hg-T-Bnz	-	Violet
T-Zn-T	Blue	Blue	T-Zn-T-Bnz	Blue	Green
T-Ag-T	Yellow	-	T-Ag-T-Bnz	-	-
T-Ni-T	-	-	T-Ni-T-Bnz	-	-
T-Pd-T	-	-	T-Pd-T-Bnz	-	-
T-Pt-T	Orange	-	T-Pt-T-Bnz	-	-
T-M-A	B.L	A.L	T-M-A-Bnz	B.L	A.L
T-A	-	-	T-A-Bnz	-	-
T-Hg-A	Blue	Green	T-Hg-A-Bnz	Blue	Green
T-Zn-A	Yellow	Red	T-Zn-A-Bnz	Red	-
T-Ag-A	Red	-	T-Ag-A-Bnz	-	-
T-Ni-A	-	Blue	T-Ni-A-Bnz	-	Blue
T-Pd-A	-	-	T-Pd-A-Bnz	-	-
T-Pt-A	-	-	T-Pt-A-Bnz	-	-
A-M-T	B.L	A.L	A-M-T-Bnz	B.L	A.L
A-T	-	-	A-T-Bnz	-	Violet
A-Hg-T	Blue	Green	A-Hg-T-Bnz	Violet	Green
A-Zn-T	Yellow	Red	A-Zn-T-Bnz	Red	Red
A-Ag-T	Red	-	A-Ag-T-Bnz	-	-
A-Ni-T	-	Blue	A-Ni-T-Bnz	Violet	Red
A-Pd-T	-	-	A-Pd-T-Bnz	-	-
A-Pt-T	-	-	A-Pt-T-Bnz	-	-

B.L: Before luminescence; A.L: After luminescence

Table S6. The complexation energies of C-G and C-C base pairs with metal cations (Kcal/mol).

Base Pairs	Energy Values						
	ΔE	ΔG	ΔH	Base Pairs	ΔE	ΔG	ΔH
C-G → C-Hg-G	−137.74	−140.33	−135.80	C-C → C-Hg-C	−88.10	−91.33	−85.90
C-G → C-Zn-G	−62.16	−63.55	−60.06	C-C → C-Zn-C	−81.07	−82.22	−79.56
C-G → C-Ag-G	−75.82	−77.77	−75.10	C-C → C-Ag-C	−93.00	−94.27	−89.90
C-G → C-Ni-G	−151.04	−154.64	−149.86	C-C → C-Ni-C	−108.75	−110.01	−107.00
C-G → C-Pd-G	−97.76	−101.04	−95.55	C-C → C-Pd-C	−77.42	−80.00	−76.20
C-G → C-Pt-G	−110.26	−113.36	−109.55	C-C → C-Pt-C	−79.55	−79.88	−76.59

Table S7. The complexation energies of C-G -Bnz and G-C-Bnz base pairs with metal cations (Kcal/mol).

Base Pairs	Energy Values						
	ΔE	ΔG	ΔH	Base Pairs	ΔE	ΔG	ΔH
C-G-Bnz → C-Hg-G-Bnz	−124.05	−125.05	−123.86	G-C-Bnz → G-Hg-CBnz	−130.99	−132.45	−128.94
C-G-Bnz → C-Zn-G-Bnz	−61.04	−61.04	−58.97	G-C-Bnz → G-Zn-C-Bnz	−66.11	−69.01	−64.89
C-G-Bnz → C-Ag-G-Bnz	−73.24	−73.24	−73.00	G-C-Bnz → G-Ag-C-Bnz	−79.05	−81.34	−78.22
C-G-Bnz → C-Ni-G-Bnz	−147.69	−147.69	−146.11	G-C-Bnz → G-Ni-C-Bnz	−148.27	−150.09	−148.00
C-G-Bnz → C-Pd-G-Bnz	−94.26	−94.26	−92.50	G-C-Bnz → G-Pd-C-Bnz	−96.13	−99.58	−94.99
C-G-Bnz → C-Pt-G-Bnz	−104.97	−104.97	−104.00	G-C-Bnz → G-Pt-C-Bnz	−108.60	−110.78	−108.01

Table S8. The complexation energies of C-C-Bnz base pairs with metal cations (Kcal/mol).

Base Pairs	Energy Values		
	ΔE	ΔG	ΔH
C-C-Bnz→ C-Hg-CBnz	−130.99	−132.45	−128.94
C-C-Bnz→ C-Zn-C-Bnz	−66.11	−69.01	−64.89
C-C-Bnz→ C-Ag-C-Bnz	−79.05	−81.34	−78.22
C-C-Bnz→ C-Ni-C-Bnz	−148.27	−150.09	−148.00
C-C-Bnz→ C-Pd-C-Bnz	−96.13	−99.58	−94.99
C-C-Bnz→ C-Pt-C-Bnz	−108.60	−110.78	−108.01

Table S9. The colour changes of of C-G, G-C, C-C and their complexes with Bnz and metal cations.

C-M-G	B.L	A.L	C-M-G-Bnz	B.L	A.L
C-G	-	-	C-G-Bnz	-	-
C-Hg-G	-	Blue	C-Hg-G-Bnz	-	Blue
C-Zn-G	Green	Green	C-Zn-G-Bnz	-	-
C-Ag-G	-	-	C-Ag-G-Bnz	-	-
C-Ni-G	-	Green	C-Ni-G-Bnz	-	-
C-Pd-G	Blue	Green	C-Pd-G-Bnz	Blue	Green
C-Pt-G	Blue	-	C-Pt-G-Bnz	Violet	Red-
G-M-C	B.L	A.L	C-M-G-Bnz	B.L	A.L
G-C	-	-	G-C-Bnz	-	-
G-Hg-C	-	Blue	G-Hg-C-Bnz	-	Yellow
G-Zn-C	Green	Green	G-Zn-C-Bnz	-	-
G-Ag-C	-	-	G-Ag-C-Bnz	-	-
G-Ni-C	-	Green	G-Ni-C-Bnz	-	Violet
G-Pd-C	Blue	Green	G-Pd-C-Bnz	Blue	Green
G-Pt-C	Blue-	--	G-Pt-C-Bnz	Violet	Orange-
C-M-C	B.L	A.L	C-M-C-Bnz	B.L	A.L
C-C	-	Violet	C-C-Bnz	-	-
C-Hg-C	Red	-	C-Hg-C-Bnz	Red	-
C-Zn-C	-	-	C-Zn-C-Bnz	-	-
C-Ag-C	Red	-	C-Ag-C-Bnz	Red	-
C-Ni-C	Violet	-	C-Ni-C-Bnz	Violet	Orange
C-Pd-C	-	-	C-Pd-C-Bnz	-	-
C-Pt-C	-	-	C-Pt-C-Bnz	--	-